Properties Evaluation of $Fe_{95-x}Si_5Ni_x$ Under the Earth's Inner-Core Conditions: Insight from the Ab-Initio Investigation

Mustapha Zidane (mustapha_zidane@um5.ac.ma)
Mohammed V Agdal University: Universite Mohammed V de Rabat
El Mehdi Salmani
Mohammed V Agdal University: Universite Mohammed V de Rabat
Meryem Elmoulat
Mohammed V Agdal University: Universite Mohammed V de Rabat
Hamid EZ-ZAHRAOUY
Mohammed V Agdal University: Universite Mohammed V de Rabat
Abdelilah Benyoussef
Mohammed V Agdal University: Universite Mohammed V de Rabat

Research Article

Keywords: Electrical resistivity, Earth's Inner core, SPR-KKR, Fe-Si-Ni, Pressure, and Temperature.

Posted Date: July 12th, 2021

DOI: https://doi.org/10.21203/rs.3.rs-667030/v1

Abstract

In this article we investigate under the same Earth's core conditions, the structural, electronic, and transport properties of Fe-Si-Ni ternary alloys based on Fe and 5% of Si with various concentrations 0%, 15%, 25%, and 40% of element Ni, by means of First-principles calculations. Based on Functional Density Theory (DFT). The Local Density Approximation (LDA) also has been adopted for the potential exchange correlation. We perform the calculation of electronic property at 360 GPa using the software Akai-KKR (machikaneyama), which used the Korringa-Kohn-Rostoker method along with coherent potential approximation (KKR-CPA). Afterward, we calculate the electrical resistivity of impurities formed on the Kubo-Greenwood formula with the vertex correction using SPR-KKR code, which is based on the relativistic polarized spin method. Then, we model the thermal conductivity by electrical resistivity for both varying in the range of 320–360 GPa and 4500-6000k of pressure and temperature, respectively; according to the conditions of the Earth's inner core ICB using Wiedemann-Franz law. Hence, our results suggest that 85–115 μΩ·cm at 0 K and 320–360 GPa, then 225–285 μΩ·cm at 4500–6000 K and 360 GPa for electrical resistivity, and then 45–55 $W \cdot m^{-1} \cdot K^{-1}$ at 4500–6000 K and 360 GPa of thermal conductivity of Earth's inner core. Lastly, the thermal and compositional convection is one of the major factors of global magnetic field that is generated by geodynamo driven.

1. Introduction

Geophysics is a branch of the Earth Sciences that not only examines the internal core of our planet, but also all the seismic, electrical, thermal, and magnetic phenomena that occur on its surface and its surrounding. As matter of fact, these processes are measured by multiple experimental approaches by means of physically measurable parameters such as density, electrical resistivity…etc. For instance, electrical prospection is one of these methods based upon determining electrical resistivity and thermal conductivity under specific conditions of high temperature and pressure, in order to understand the lithological formation as well as the mineralization of the Earth's core.

Multiple studies indicate that the internal structure of the Earth is made up of different chemical elements with different percentages. It was found that the most dominant element in Earth's core is iron with a slight change in percentages of lighter elements such as Ni, Si, S, N, O, C, H, and Mg (McDonougha and Suna. 1995). The Iron is abounded in nature in three structures, which are Face-Centered Cubic (FCC), Hexagonal-Close-Packed (HCP) (Mathon et al., 2004), and Body Centered Cubic (BCC) (Belonoshko and Ahuja, 2003; Luo et al., 2010). However, the HCP structure is the most stable one in the conditions of high temperature and pressure of iron in the Earth's core. Indeed, in order to better investigate the structure of the Earth's inner core, it is necessary to study the saturation of electrical resistivity and thermal conductivity of the structure of HCP of iron or iron doped by different alloys of elements existed in the heart of the Earth under high temperature and pressure. In the literature, several studies suggested that the saturation of the electrical resistivity of the outer and the inner cores was approximately equal to 1×10^{-6} Ω.m. This saturation of electrical and thermal conductivity was studied by many researchers (Gomi et al. 2013, 2016; Kiarasi and Secco, 2015; Ohta et al. 2016, 2018; Pozzo and Alfè.

2016; Wagle et al. 2018; Xu et al. 2018, Zidane et al.2020). During the last decade, many publications revealed that the estimations of the electrical resistivity of pure, binary, and ternary systems based on iron such as experimental works that examine the electrical resistivity of Fe with the presence of Si, Ni, S, and C (Gomi et al. 2013, 2016; Seagle et al. 2013; Gomi and Hirose 2015; Kiarasi and Secco 2015; Suehiro et al. 2017; Ohta et al.2018; Zhang et al. 2018). Moreover, other researchers have studied the effects of alloying based on iron with a few light elements like Si, O, and S by using First-Principles Molecular Dynamics (FPMD) (de Koker et al. 2012; Pozzo et al. 2013, 2014; Wagle et al. 2018). Furthermore, there were other investigators performing theoretical calculations (de Koker et al. 2012; Pozzo et al.2012, 2013; Gomi et al. 2013, 2016; Gomi and Yoshino. 2018; Drchal et al. 2018; Zidane et al. 2020) for comparing it with the experimental results.

In sundry previous theoretical and experimental works, the electrical resistivity was experimentally estimated for the binary alloys based on iron, which are $3.62–4.65\times10^{-6}$ Ωm (Stacey and Loper, 2007), $1.25–0.46\times10^{-6}$ Ωm for Fe + (Ni, Si) (Gomi et al. 2016), $1.02–0.22\times10^{-6}$ Ωm for Fe + light elements (Ni, Si, N, S, C, O) (Gomi and Yoshino 2018), and $0.6–0.25\times10^{-6}$ Ωm for Fe + (Ni, O, S, Si) (Drchal et al. 2018). In addition to that, there are also some experimental estimations to benchmark them with, like $1.5–2.1\times10^{-6}$ Ωm (Seagle et al. 2013), $0.55–1.09\times10^{-6}$ Ωm (Gomi et al. 2013), and $0.60–1.10\times10^{-6}$ Ωm (Gomi and Hirose 2015). Gomi and Hirose 2015 conducted on ternary alloys based on Fe, who found out that the electrical resistivity was 1.04×10^{-6} Ωm for pressure 135 GPa and 8.44×10^{-7} Ωm for 330 GPa of $Fe_{67.5}Ni_{10}Si_{22.5}$. At the core-mantle boundary (CMB) condition, Stacey and Anderson 2001 reported the estimation of electrical resistivity of $Fe_{65}Ni_{10}Si_{25}$ to be 2.12×10^{-6}Ωm. There was also some theoretical study of $Fe_{90-x}Ni_{10}Si_x$ (X = 5, 10, 15, 20, 25, 30) of Gomi et al. 2016 and $Fe_{90-x}Ni_{10}Si_x$ (X = 2, 4, 5, 10, 15, 20, 25, 30, 40, 50) of Zidane et al. 2020 with different value of pressure. The electrical resistivity and thermal conductivity are proportional between them according to Wiedemann–Franz law:

$$k = \frac{LT}{\rho(T)} \qquad (1)$$

where k is thermal conductivity in W/ (K.m), $L = 2.45\times10^{-8}$ W.Ω/K^2 is the Lorenz number, T is temperature in K°, and ρ is electrical resistivity in Ωm.

In this present research article, we performed first-principles calculations based on Functional Density Theory (DFT) for ternary $Fe_{0.95-x}Si_{0.05}Ni_x$ alloys by X=15%, 25%, 40% and binary $Fe_{0.95}Si_{0.05}$ alloy under conditions of Earth's inner core. Our theoretical calculation are electronic properties and the electrical resistivity that were performed at high pressure. We also calculated the thermal conductivity by using the Wiedemann-Franz equation. Afterward, we discussed the implication of thermal conductivity of iron doped by silicon and nickel for the explanation of heat transport and its possible loss on Earth.

2. Computational Details

In these first-principles calculations, we relaxed the binary structure $Fe_{0.95}Si_{0.05}$ and ternary structure $Fe_{0.95-x}Si_{0.05}Ni_x$ with 15%, 25%, 40%. We calculated the electronic properties by using the AkaiKKR (MACHIKANEYAMA) package coded by Akai (1989). This calculation adopts Coherent Potential Approximation (CPA) (Butler, 1985), which employs the Local Density Approximation (LDA) based on Korringa–Kohn–Rostoker (KKR) and the Green function method with the Atomic Sphere Approximation (ASA) that was combined to exchange-correlation potential (Moruzzi et al., 1978). In addition, we employed the scalar relativistic approximation and the angular momentum quantum number l to calculate the wave functions up to 3, i.e., s, p, d, and f orbitals. Afterwards, we computed the electrical resistivity from the Kubo–Greenwood formula (Greenwood, 1958; Kubo, 1957) by using the SPR-KKR-package (spin-polarized relativistic Korringa-Kohn-Rostoker) (Ebert et al., 2011), which is based on KKR-Green's function method and limited to the Atomic Sphere Approximation (ASA) along with the Local Density Approximation (LDA).

In the current study, we focused on calculating the average value of the electrical resistivity by using the equation $\rho = (2\rho_{\perp} + \rho_{||})/3,$ where $\rho_{\perp}$ and $\rho_{||}$ are the resistivities calculated perpendicular and parallel to the c-axis. Through the thermal conductivity of the Earth's core, the moving electrons mainly transported the heat in the metals. Thus, we can estimate this thermal conductivity of the Earth's core from the electrical resistivity by using the Wiedemann-Franz law indicated in the equation (1).

3. Results And Discussions

3.1. Structural properties

We know that Fe is the most dominant element in the inner core of the Earth based on the HCP structure, which is the most stable structure of 20 GPa. Therefore, in our work all the calculations are carried out with this last structure based on a space group of $P6_3/mmc$ (N°194) (Zidane et al., 2020). The unit cell of HCP structure of iron is containing two atoms that occupy the Wyckoff position 2(c) in the following positions Fe: (1/3, 2/3, 1/4); (2/3, 1/3, 3/4) (Takahashi et al., 1968).

We have calculated the volume at 320, 330, 340, 350, and 360 GPa for four structures doped by 0%, 15%, 25%, and 40% of Ni in the $Fe_{0.95-x}Si_{0.05}Ni_x$ alloys of hcp structure (Figure 1). For all structures, we observe the decreasing of volumes related to the pressure. The decrement in the volume is almost linear in the interval (320-360) GPa. We also notice that the volume of $Fe_{0.95}Si_{0.05}$ binary alloy is lower than the one of the other systems ternary alloys. This volume of systems $Fe_{0.95-x}Si_{0.05}Ni_x$ is increasing with the increase of Ni concentration.

3.2. Electronic properties

We have performed the calculation for nonmagnetic HCP Fe-Si, and Fe-Si-Ni alloys of the Density of States (DOS), the electronic band structures, and Fermi Surface.

In Figure 2 we calculated the electronic Density of States (DOS) at about 360 GPa of pressure for nonmagnetic $Fe_{0.95-x}Si_{0.05}Ni_x$ (x = 0, 15, 25, and 40%). The metallicity is confirmed for binary structure and all ternary structures. Nevertheless, we noticed a decrease in DOS at the Fermi level as the concentration of impurities increases at the expense of iron atoms with conserving the Si concentration fixed at 5% and other concentration 0%, 15%, 25%, 40% of Ni.

The decrease in density at the Fermi level with the increasing of the dopant content of Ni in Fe-Si has been explained by the electronegativity of silicon and nickel impurities, which is higher than that of iron. Therefore, the multiplicity may continue to decrease, and the DOS will lower when the iron atoms are replaced by other atoms of higher electronegativity. Additionally, the surface under the DOS widens with the increase in light elemental impurities, which has been explained by the number of valence electrons that occupies this surface.

The electronic band structure proves the metallicity of all alloys for 360 GPa (Figure. 3). The all-dispersion profiles are very similar. Concerning the energies of the bands, there are small changes with increasing doping concentration. At low or null concentration of doping Ni in Fe with the Si concentration fixed at 5%, the energy bands show sharp bands and similar to that of a perfectly ordered crystal. On the contrary, they become more smeared at high dopant concentration as we have in the DOS graph for the Fe-Si based alloys. In addition, the electronic energy bands are widening with the energy uncertainty that defines by the of energy over time as $\Delta E\, \Delta t \geq \hbar/2$ where:

is the uncertainty of energy.

Δt: is the lifetime of the electron.

$\hbar$: is the reduced Planck constant.

Since the electrical resistivity is proportionally inversed to electronic density, we have explained the DOS by the reliant of disorder thermic. Thus, the band structure is justified by the escalation of the crossing bands at the Fermi level.

The cross-sections of the Fermi energy of the Bloch spectral function were presented for the same binary and ternary structures at 360 GPa based on Fe-Si (Figure 4). These cross-sections have to be low at high percentage of impurities from Ni in Fe-Si. Moreover, it seems an acceptable display for small or null percentages of Ni. The saturation of the electrical resistivity of alloys and transition metals occurs at very high resistivity (Mooij, 1973; Bohnenkamp et al., 2002). This latter was produced when the interatomic distance fit the mean of free path of conduction electrons. We call this condition the Mott-Ioffe-Regel criterion (Mott, 1972; Gurvitch, 1981), which also can be defined from the Bloch Spectral Function (BSF) at the Fermi energy (Figure 4), because the width of the enlargement of the Fermi surface is varied inversely proportional at the mean free path. The inverse of the mesh parameter also is proportional at the edge of the first Brillouin zone (Butler and Stocks, 1984; Gomi et al., 2016; Zidane et al., 2020).

3.3. Electrical resistivity

There are several experiments with dilute alloys that measured their electrical resistivity conducted by Norbury in 1920. This author noticed a horizontal increase in term of distance between host metal in the periodic table and the positions of the impurity element. We know in the Earth's core that the values of pressure and temperature proportionally increase with depth. As a matter of fact, in the inner core of the Earth, the values of pressure vary from 320 to 360 GPa and the temperature from 4500 to 6000 k. By using the Kubo-Greenwood method, we performed the calculations of electrical resistivity based on alloy $Fe_{0.95-x}Si_{0.05}Ni_x$ doped with some percentage 0%, 15%, 25%, and 40% of Ni alloys at high-pressure values, which are 320, 330, 340, 350, and 360 GPa of HCP structure (Figure 5). Similarly, analysis for the HCP morphology can be found in (Zidane et al., 2020).

Generally speaking, the electrical resistivity of all the ternary $Fe_{0.80}Si_{0.05}Ni_{0.15,}$ $Fe_{0.70}Si_{0.05}Ni_{0.25}$, and $Fe_{0.55}Si_{0.05}Ni_{0.40,}$ alloys are higher than the one of the $Fe_{0.95}Si_{0.05}$ binary alloy as shown in Figure 5. The increasing order of impurity resistivity is found as Ni (15%) < Ni (25%) < Ni (40%). For this light element Ni doped in $Fe_{0.95}Si_{0.05}$, we figured out a tiny decrease in electrical resistivity from 320 to 360 GPa for binary and ternary structures, which it can be the same for all pressure points in each concentration. At 0% concentration of Ni, i.e., the binary alloy $Fe_{0.95}Si_{0.05}$ has a resistivity in the range of 53–57 μΩ·cm. At 15%, 25%, and 40% concentration of Ni, i.e., the ternary alloys $Fe_{0.80}Si_{0.05}Ni_{0.15}$, $Fe_{0.70}Si_{0.05}Ni_{0.25}$, and $Fe_{0.55}Si_{0.05}Ni_{0.40,}$ and their resistivity are 88–92 μΩ·cm, 99–103 μΩ·cm, and 111–114 μΩ·cm, respectively.

The vibration modes harden along with increase in the pressure. In other term, when the phonons harder, this leads to a coupling decrease between the electron and phonons. This coupling is directly proportional to the electrical resistivity. In explanation, the electrical resistivity drops, because of the absence of structural, electronic, and/or topological transition, which was due to the increase in pressure. From phonons perspective, Lanzillo et al. (2014) discussed this outcome in term of the effect of pressure on resistivity. As a benchmark with theoretical results that were calculated at 0 K, we confirm that our findings are in a great agreement with others' works such as 62-66 μΩ·cm of $Fe_{0.85}Ni_{0.10}Si_{0.05}$, 100-102 μΩ·cm of $Fe_{0.75}Ni_{0.10}Si_{0.15}$ and 115-118 μΩ·cm of $Fe_{0.65}Ni_{0.10}Si_{0.25}$ including pressure (Zidane et al. 2020). Our values of electrical resistivity at 360 GPa are bigger than the one of 42 μΩ·cm of $Fe_{0.85}Ni_{0.10}Si_{0.05}$, 78 μΩ·cm of $Fe_{0.75}Ni_{0.10}Si_{0.15}$ and 95 μΩ·cm of $Fe_{0.65}Ni_{0.10}Si_{0.25}$ at 120 GPa (Gomi et al. 2016). All the previous calculations of volume, density electronic, band structure, Bloch spectral function, and electrical resistivity were received at 0 K of temperature by using the Functional Density Theory (DFT).

In the context of electrical resistivity as a function of temperature, the electrical resistivity of hcp-$Fe_{0.95-x}Si_{0.05}Ni_x$ (x = 0%, 15%, 25%, and 40%) alloys were calculated at fixed pressure 360 GPa and within range of temperature 4500-6000 K, which are the inner core conditions P-T of ICB. In figure 6, we observed for the all-last alloys an increase between 225 μΩ·cm and 285 μΩ·cm of the electrical resistivity as a function of temperature. Consequently, the electrical resistivities get closer to each other, and then converge to a

single point at very high temperature; because these structures are depressed under very high conditions of pressure-temperature. Furthermore, we also notice an increase in the electrical resistivity with increasing of Ni percentage doped in $Fe_{0.95}Si_{0.05}$ for all the points of temperatures as 4500 k, 4750 k, 5000 k, 5250 k, 5500 k, 5750 k, and 6000 k.

In the conditions of the Earth's inner core, we modeled the electrical resistivity for HCP structure for $Fe_{0.95-x}Si_{0.05}Ni_x$ (x = 0%, 15%, 25%, and 40%), which is bigger than the measurement of hcp-Fe-5Ni-4Si and hcp-Fe-5Ni-8Si at 2000-4500 K and 140 GPa of CMB in a diamond-anvil cell (DAC) (Zhang et al. 2021). Regarding the hcp-Fe-4Si at 99 GPa and up to 1900 K are also by the diamond-anvil cell (Inoue et al., 2020). As a general agreement, the pressure and temperature of the CMB are less than that of ICB. Thus, this outcome makes a perfect sense because the electrical resistivity increases with temperature.

According to the literature, there are many studies found that the estimations of electrical resistivity by the method diamond-anvil cell, such as 102 μΩ·cm for CMB and 82 μΩ·cm for ICB of $Fe_{77.5}Si_{22.5}$ (Gomi et al., 2013), 104 μΩ·cm for CMB and 84.4 μΩ·cm for ICB of $Fe_{67.5}Ni_{10}Si_{22.5}$ (Gomi et al., 2015), under the conditions of the core-mantle boundary (CMB; 135 GPa, 3750 K), and inner core boundary (ICB; 330 GPa, 4971 K) respectively. Gomi et al., 2016 concluded that the collapse of the large portion of the Fermi surface by using Matthiessen's rule could violate at higher Si contents from 1 to ∼ 9 wt.% in the Fe-Si structure. Under the selected for the present study and the ones of the Earth's inner core, which are 330–360 GPa of pressure and 5000–7000 K of temperature, the values of resistivity are between 0.7 and 1.5 $\times 10^{-6}$ Ωm (Pozzo and Alfè. 2016). Other authors used binary and ternary system based on iron with some element C, O, S, H, N, Ni at first principal calculations such as (de Koker et al., 2012; Xu et al., 2018; Pozzo et al., 2012); to that we would like to add the experiments of basic principles of Shock Compression in the condition of inner earth's core conducted by (Matassov, 1977).

3.4. Thermal conductivity

In this part of our reach, we converted the electrical resistivity (ρ) to thermal conductivity (k) by using the Wiedemann-Franz law (Equation 1) at pressure and temperature condition of Earth's core. Hence, we carried out all our calculation the thermal conductivity at fixed pressure 360 GPa and in the range 4500-6000 k of temperature for 0%, 15%, 25% and 40% concentration of Ni in alloys based of Fe+5at%Si **(Figure.7).**

Figure.7 indicates, on one hand, the thermal conductivity that increases with an increase of temperature for all our last structures in the range of 45-55 $W{\cdot}m^{-1}{\cdot}K^{-1}$. On the other hand, this latter increases with the decrease of concentration of Ni doped in $Fe_{0.95}Si_{0.05}$ system. Our result values of thermal conductivity at the Earth inner's core conditions are in good agreement with other studies such as Stacey and Anderson, 2001 who obtained 46 $W{\cdot}m^{-1}{\cdot}K^{-1}$ for CMB and 63 $W{\cdot}m^{-1}{\cdot}K^{-1}$ for ICB. Stacey and Loper, 2007 obtained 28.3 $W{\cdot}m^{-1}{\cdot}K^{-1}$ with slight variation in increase of depth for Fe-Ni-Si. In addition, Zhang et al., 2021 acquired the thermal conductivity in the range 2000-4500 k and 140 GPa under the conditions of Earth's

outer core at 40-75 $W \cdot m^{-1} \cdot K^{-1}$. In contrast, other investigators received higher values of thermal and electrical conductivity than ours (de Koker et al. 2012; Ohta et al. 2016; Pozzo et al. 2012, 2014).

4. Conclusion

In this scientific article, we used the ab initio method of functional density theory to calculating the structural, electronic, and transport proprieties of hcp-Fe0.95-xSi0.05Nix with 0%, 15%, 25%, and 40% of Ni alloys in the ranges 320-360 GPa and 4500-6000 k as the conditions of pressure and temperature as the Earth's inner core. We calculated the electrical resistivity of all structures by using the Kubo-greenwood formula (Butler 1985; Oshita et al. 2009). Afterward, we determined the thermal conductivity by applying Weidman Franz law in the ICB conditions. Consequently, our findings of the electrical resistivity and the thermal conductivity calculations of Fe-Si-Ni alloys are consistent with the ones found by our predecessors like (Stacey and Anderson, 2001; Stacey and Loper, 2007; and Zhang et al., 2021). At the end, we would like to join the consensus of the geodynamo that has been driven by thermal convection in the Erath's inner core that the values of thermal conductivity should be low. As well as said by Korte[1], "these physical properties are not exactly known because we cannot just go down to the Earth's core and directly measure them." Nevertheless, she mentioned, "they have to be inferred." Throughout this work, we affirm this inference and corroborate previous threshold of the thermal conductivity of the Earth's inner core, which remains at lower values. [1] Monika Korte (0000-0003-2970-9075) - ORCID | Connecting Research and Researchers

References

1. Akai, H., 1989. Fast Korringa-Kohn-Rostoker coherent potential approximation and its application to FCC Ni-Fe systems. J. Phys. Condens. Matter 1, 8045–8063.
2. Belonoshko, A.B., Ahuja, R., 2003. Stability of the body-centred-cubic phase of iron in the Earth's inner core. Nature 424, 1032–1034.
3. Bohnenkamp, U., Sandstrom, R., 2002. Electrical resistivity of steels and face-centered-cubic iron. J. Appl. Phys. 92, 4402–4407. https://doi.org/10.1063/1.1502182.
4. Butler, W.H., 1985. Theory of electronic transport in random alloys: Korringa-Kohn-Rostoker coherent-potential approximation. Phys. Rev. B 31, 3260–3277.
5. Butler, W.H., Stocks, G.M., 1984. Calculated electrical conductivity and thermopower of silver-palladium alloys. Phys. Rev. B 29, 4217–4223.
6. de Koker, N., Steinle-neumann, G., 2012. Electrical resistivity and thermal conductivity of liquid Fe alloys at high P and T , and heat flux in Earth's core. Proc. Natl. Acad. Sci. 109, 4070–4073. https://doi.org/10.1073/pnas.1111841109.
7. Ebert, H., Kodderitzsch, D., Minar, J., 2011. Calculating condensed matter properties using the KKR-Green's function method — recent developments and applications. Reports Prog. Phys. 74, 096501. https://doi.org/10.1088/0034-4885/74/9/096501.

8. Inoue, H., Suehiro, S., Ohta, K., Hirose, K., Ohishi, Y., 2020. Resistivity saturation of hcp Fe-Si alloys in an internally heated diamond anvil cell: a key to assessing the Earth's core conductivity. Earth Planet. Sci. Lett. 543, 116357.
9. Kiarasi, S., Secco, R.A., 2015. Pressure-induced electrical resistivity saturation of Fe17Si. Phys. status solidi b 252, 2034–2042. https://doi.org/10.1002/pssb.201552029.
10. Kubo, R., 1957. Statistical-Mechanical Theory of Irreversible Processes. J. Phys. Soc. Japan 12, 570–586.
11. Matassov, G., 1977. The Electrical Conductivity of Iron-Silicon Alloys at High Pressures and the Earth's Core. University of California, Livermore, California, p.180.
12. Mathon, O., Baudelet, F., Itie, J.P., Polian, A., Astuto, M., Chervin, J.C., Pascarelli, S., 2004. Dynamics of the Magnetic and Structural α-ε Phase Transition in Iron. Phys. Rev. Lett. 93, 255503. https://doi.org/10.1103/PhysRevLett.93.255503
13. McDonough W. F. and Sun S. S. (1995) The composition of the Earth. Chem. Geol. 120, 223–253.
14. Mooij, J.H., 1973. Electrical Conduction in Concentrated Disordered Transition Metal Alloys. Phys. Status Solidi 17, 521.
15. Mott, N.F., 1972. The electrical resistivity of liquid transition metals. Philos. Mag. 26, 1249–1261.
16. Moruzzi, V.L., Janak, J.F., Williams, A.R., 1978. Calculated Electronic Properties of Metals. Pergamon Press Inc., New York. https://doi.org/10.1016/B978-0-08-022705-4.50001-6.
17. Norbury, A.L., 1920. The Electrical Resisitivity of Dilute Metallic Solid Solutions. Trans. Faraday Soc. 16, 570–596.
18. Lanzillo, N.A., Thomas, J.B., Watson, B., Washington, M., Nayak, S.K., 2014. Pressure-enabled phonon engineering in metals. Proc. Natl. Acad. Sci. 111, 8712–8716. https://doi.org/10.1073/pnas.1406721111.
19. Luo, W., Johansson, B., Eriksson, O., Arapan, S., Souvatzis, P., Katsnelson, M.I., Ahuja, R., 2010. Dynamical stability of body center cubic iron at the Earth's core conditions. Proc. Natl. Acad. Sci. 107, 9962–9964. https://doi.org/10.1073/pnas.1004076107
20. Gomi, H., Hirose, K., 2015. Electrical resistivity and thermal conductivity of hcp Fe – Ni alloys under high pressure : Implications for thermal convection in the Earth ' s core. Phys. Earth Planet. Inter. 247, 2–10. https://doi.org/10.1016/j.pepi.2015.04.003
21. Gomi, H., Hirose, K., Akai, H., Fei, Y., 2016. Electrical resistivity of substitutionally disordered hcp Fe – Si and Fe – Ni alloys : Chemically-induced resistivity saturation in the Earth's core. Earth Planet. Sci. Lett. 451, 51–61. https://doi.org/10.1016/j.epsl.2016.07.011
22. Gomi, H., Ohta, K., Hirose, K., Labrosse, S., Caracas, R., Verstraete, M.J., Hernlund, J.W., 2013. The high conductivity of iron and thermal evolution of the Earth's core. Phys. Earth Planet. Inter. 224, 88–103. https://doi.org/10.1016/j.pepi.2013.07.010
23. Gomi, H., Yoshino, T., 2018. Impurity Resistivity of fcc and hcp Fe-Based Alloys : Thermal Stratification at the Top of the Core of Super-Earths. Front. Earth Sci. 6, 1–22.

https://doi.org/10.3389/feart.2018.00217

24. Greenwood, D.A., 1958. The Boltzmann Equation in the Theory of Electrical Conduction in Metals. Proc. Phys. Soc. 71, 585.
25. Gurvitch, M., 1981. Ioffe-Regel criterion and resistivity of metals. Phys. Rev. B 24, 7404–7407.
26. Ohta, K., Kuwayama, Y., Hirose, K., Shimizu, K., Ohishi, Y., 2016. Resistivity of iron at Earth's core conditions. Nature 534, 95–106. https://doi.org/10.1038/nature17957
27. Ohta, K., Suehiro, S., Hirose, K., Ohishi, Y., 2018. Electrical resistivity of fcc phase iron hydrides at high pressures and temperatures. Comptes rendus Geosci. 351, 147–153. https://doi.org/10.1016/j.crte.2018.05.004
28. Pozzo, M., Alfè, D., 2016. Saturation of electrical resistivity of solid iron at Earth ' s core conditions. Springerplus 5, 256. https://doi.org/10.1186/s40064-016-1829-x
29. Pozzo, M., Davies, C., Gubbins, D., Alfe, D., 2013. Transport properties for liquid silicon-oxygen-iron mixtures at Earth's core conditions 014110, 1–10. https://doi.org/10.1103/PhysRevB.87.014110
30. Pozzo, M., Davies, C., Gubbins, D., Alfe, D., 2012. Thermal and electrical conductivity of iron at Earth's core conditions. Nature 485, 355–360. https://doi.org/10.1038/nature11031
31. Pozzo, M., Davies, C., Gubbins, D., Alfè, D., 2014. Thermal and electrical conductivity of solid iron and iron – silicon mixtures at Earth ' s core conditions. Earth Planet. Sci. Lett. 393, 159–164. https://doi.org/10.1016/j.epsl.2014.02.047
32. Seagle, C.T., Cottrell, E., Fei, Y., Hummer, D.R., Prakapenka, V.B., 2013. Electrical and thermal transport properties of iron and iron-silicon alloy at high pressure. Geophys. Res. Lett. 40, 5377–5381. https://doi.org/10.1002/2013GL057930s
33. Stacey, F.D., Anderson, O.L., 2001. Electrical and thermal conductivities of Fe–Ni–Si alloy under core conditions. Phys. Earth Planet. Inter. 124, 153–162.
34. Stacey, F.D., Loper, D.E., 2007. A revised estimate of the conductivity of iron alloy at high pressure and implications for the core energy balance. Phys. Earth Planet. Inter. 161, 13–18. https://doi.org/10.1016/j.pepi.2006.12.001
35. Suehiro, S., Ohta, K., Hirose, K., Morard, G., Ohishi, Y., 2017. The influence of sulfur on the electrical resistivity of hcp iron: Implications for the core conductivity of Mars and Earth. Geophys. Res. Lett. 44, 8254–8259. https://doi.org/10.1002/2017GL074021
36. Takahashi, T., Bassett, W.A., Mao, H., 1968. Isothermal Compression of the Alloys of Iron up to 300 Kilobars at Room Temperature : Iron-Nickel Alloys TARO. J. Geophys. Res. 73, 4717–4725.
37. Tateno, S., Hirose, K., Ohishi, Y., Tatsumi, Y., 2010. The Structure of Iron in Earth's Inner Core. Science 330, 359–362.
38. Tateno, S., Kuwayama, Y., Hirose, K., Ohishi, Y., 2015. The structure of Fe–Si alloy in Earth's inner core. Earth Planet. Sci. Lett. 418, 11–19. https://doi.org/10.1016/j.epsl.2015.02.008
39. Wagle, F., Steinle-Neumann, G., de Koker, N., 2018. Saturation and negative temperature coefficient of electrical resistivity in liquid iron-sulfur alloys at high densities from first-principles calculations.

Phys. Rev. B 97, 094307. https://doi.org/10.1103/PhysRevB.97.094307

40. Xu, J., Zhang, P., Haule, K., Minar, J., Wimmer, S., Ebert, H., Cohen, R.E., 2018. Thermal Conductivity and Electrical Resistivity of Solid Iron at Earth ' s Core Conditions from First Principles. Phys. Rev. Lett. 121, 96601. https://doi.org/10.1103/PhysRevLett.121.096601
41. V. Drchal, J. Kudrnovský, D. Wagenknecht, I.(2018), Turek, Alloy disorder and fluctuating magnetic moments in the Earth's core, Journal of Magnetism and Magnetic Materials.
42. Zidane, M., Salmani, E.M., Majumdar, A., Ez-zahraouy, H., Benyoussef, A., and Ahuja, R. (2020) Electrical and thermal transport properties of Fe – Ni based ternary alloys in the earth ' s inner core : An ab initio study. Physics of the Earth and Planetary Interiors, 301, 106465.
43. Zhang Youjun, Mingqiang Hou, Peter Driscoll, Nilesh P. Salke, Jin Liu, Eran Greenberg, Vitali B. Prakapenka, Jung-Fu Lin (2021) Transport properties of Fe-Ni-Si alloys at Earth's core conditions: Insight into the viability of thermal and compositional convection. Earth and Planetary Science Letters, 553, 116614.

Figures

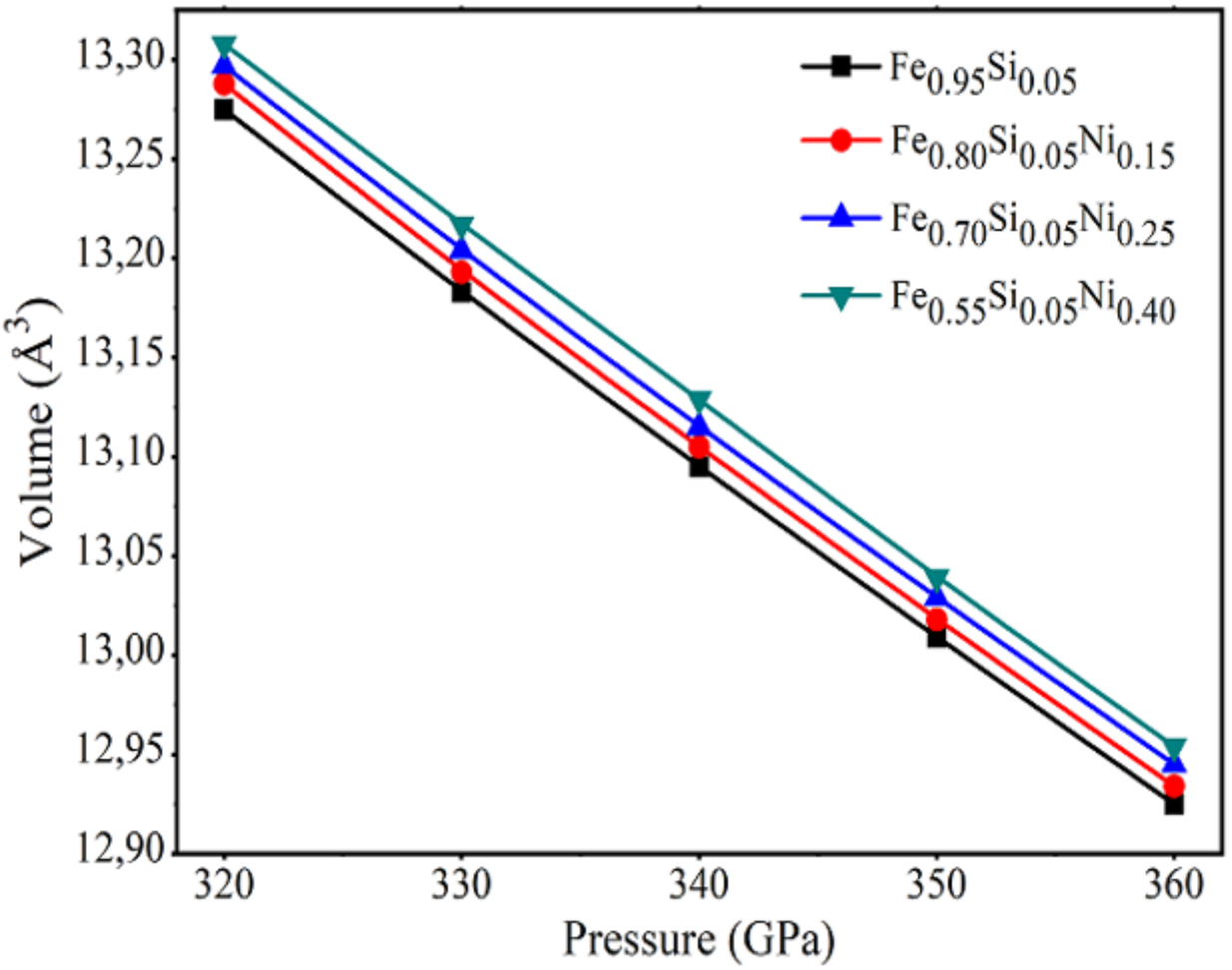

Figure 1

The Volume related to Pressure of Fe0.95-xSi0.05Nix (x = 0 ,15 ,25 and 40 %) of HCP structure.

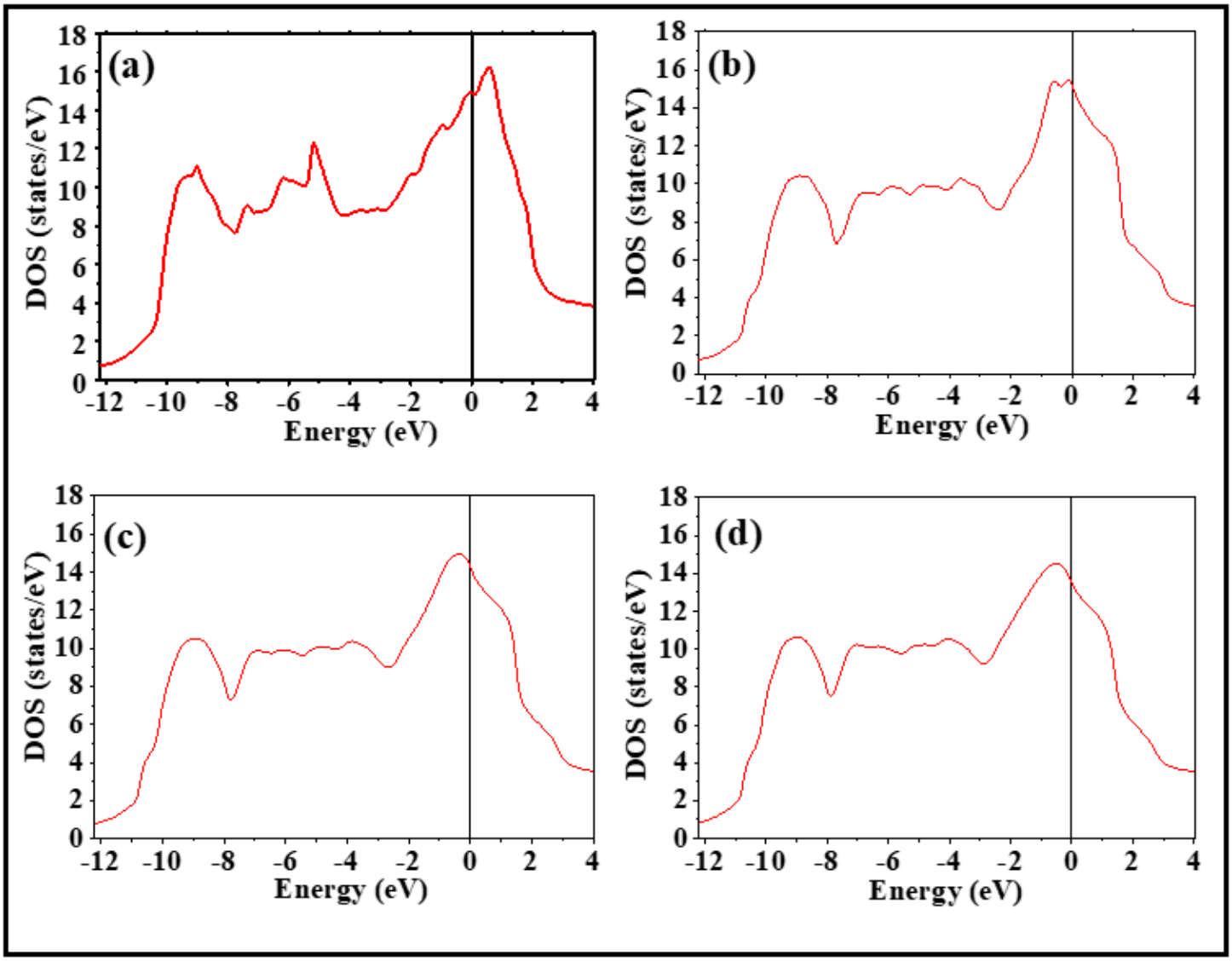

Figure 2

The Electronic Density of States (DOS) Of (a) Fe0.95Si0.05, (b) Fe0.8Si0.05Ni0.15, (c) Fe0.7Si0.05Ni0.25 and (d) Fe0.55Si0.05Ni0.4 in 360 GPa. The Fermi energy is set to be 0 eV of hcp structure.

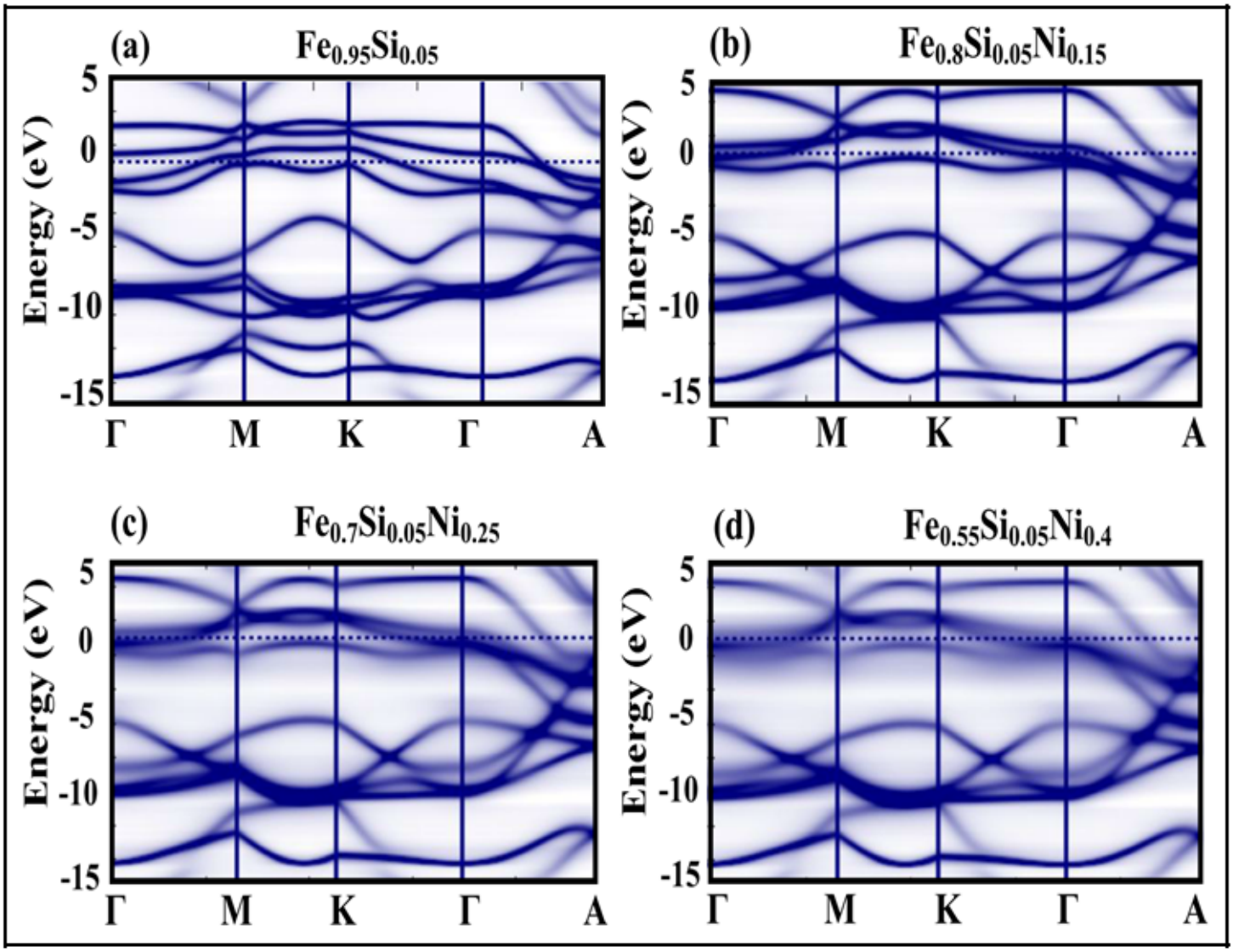

Figure 3

Electronic band structures of Fe0.95-xSi0.05Nix (x = 0 ,15 ,25 and 40 %) in 360 GPa of HCP structure.

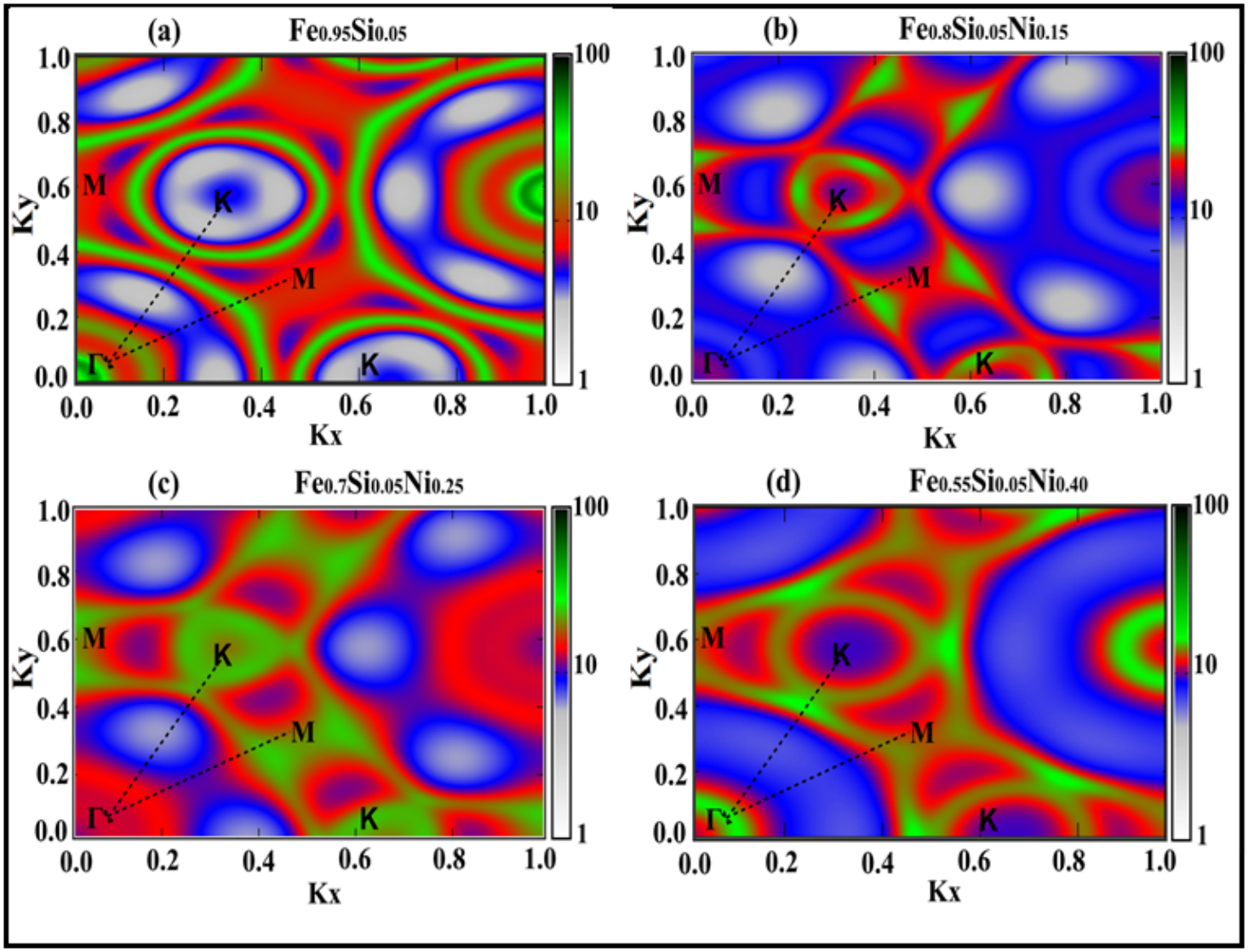

Figure 4

The cross sections of the Bloch spectral function at the Fermi level of Fe0.95-xSi0.05Nix (x = 0, 5, 15 and 25 %) in 360 GPa of HCP structure.

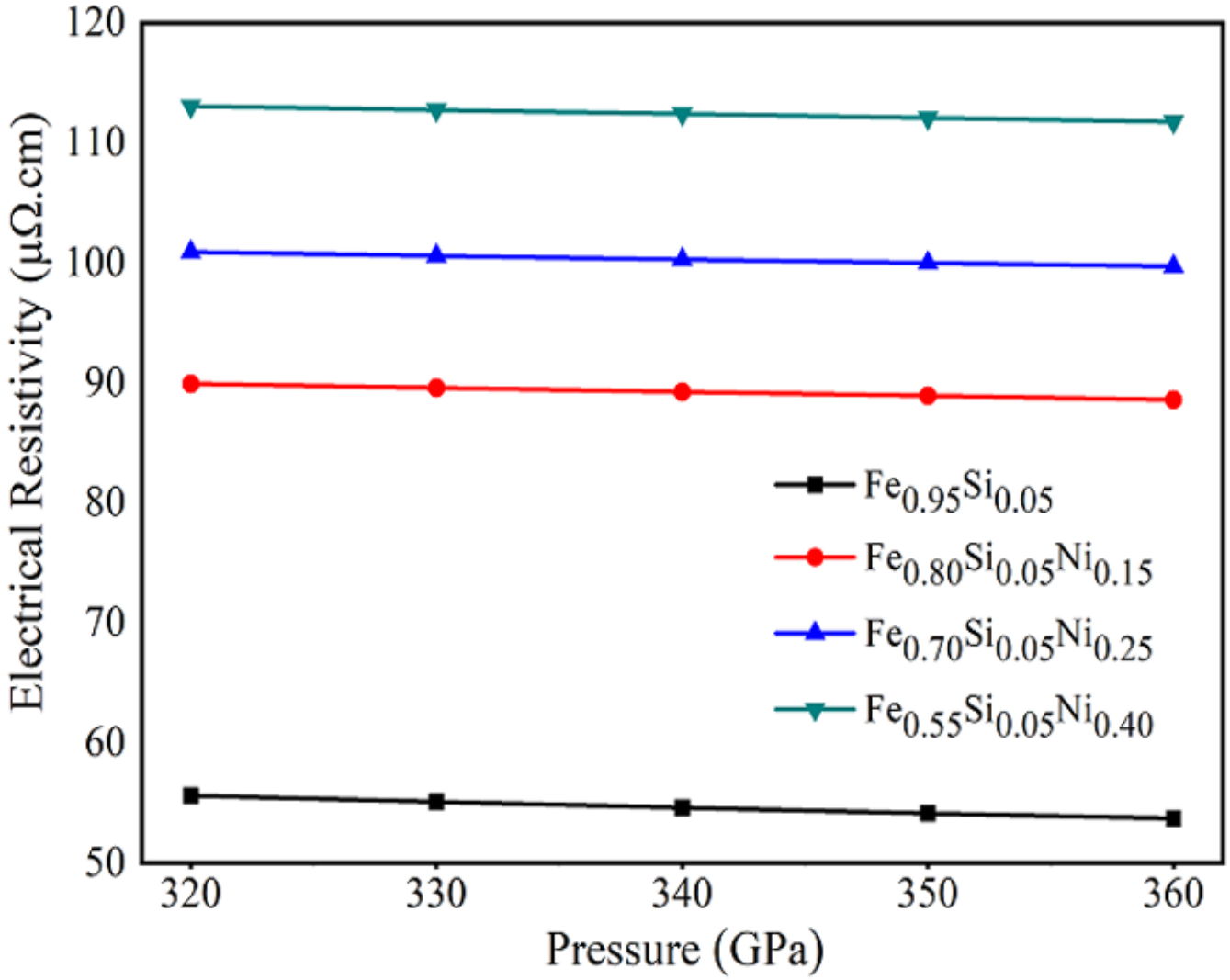

Figure 5

Electrical resistivity vs pressure for impurity concentrations of 0%, 15%, 25% and 40% of Ni doped in Fe0.95-xSi0.05Nix alloys of hcp structure at 0 k.

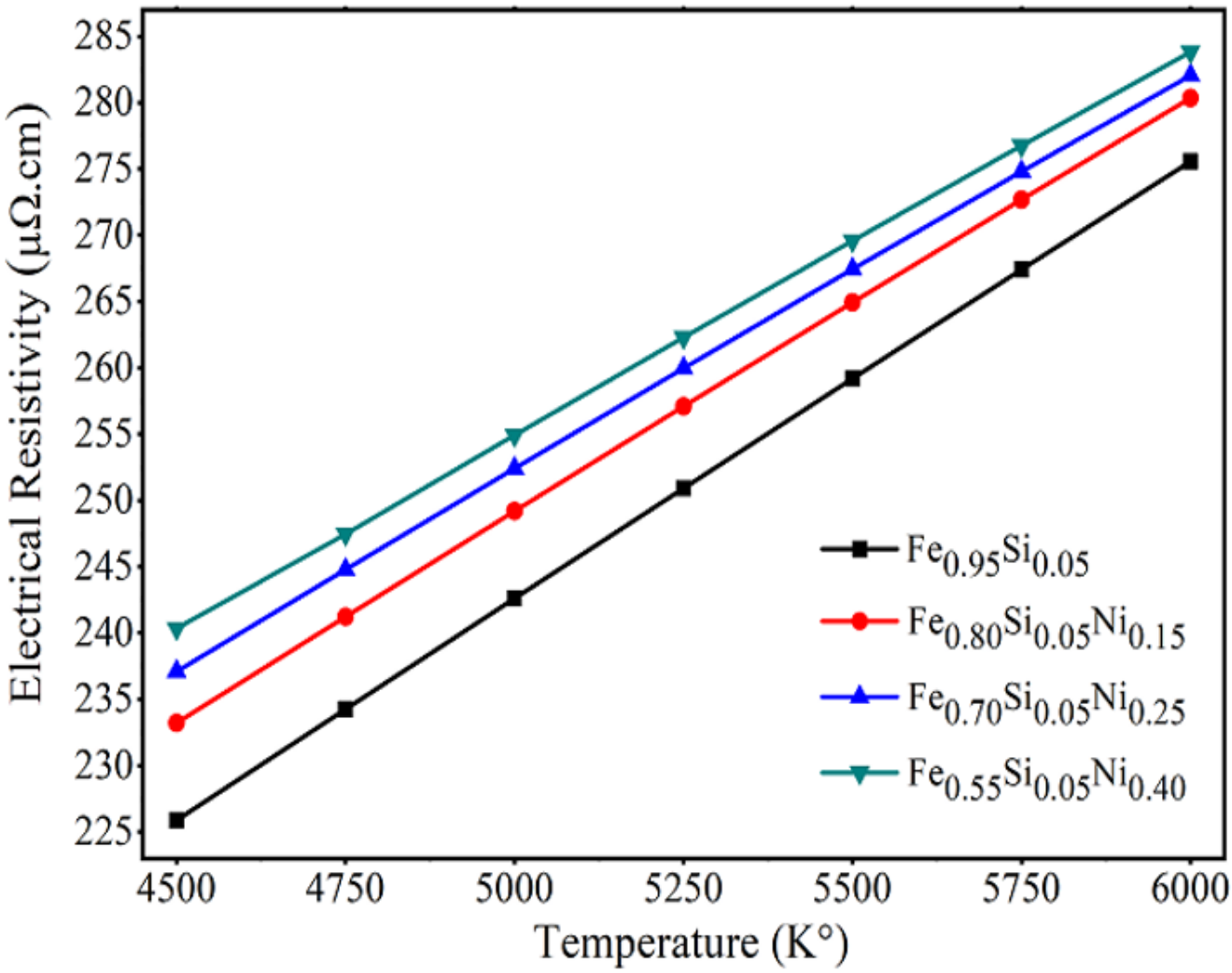

Figure 6

Electrical resistivity vs temperature at 360 GPa for impurity concentrations of 0%, 15%, 25% and 40% of Ni doped in Fe0.95-xSi0.05Nix alloys of hcp structure.

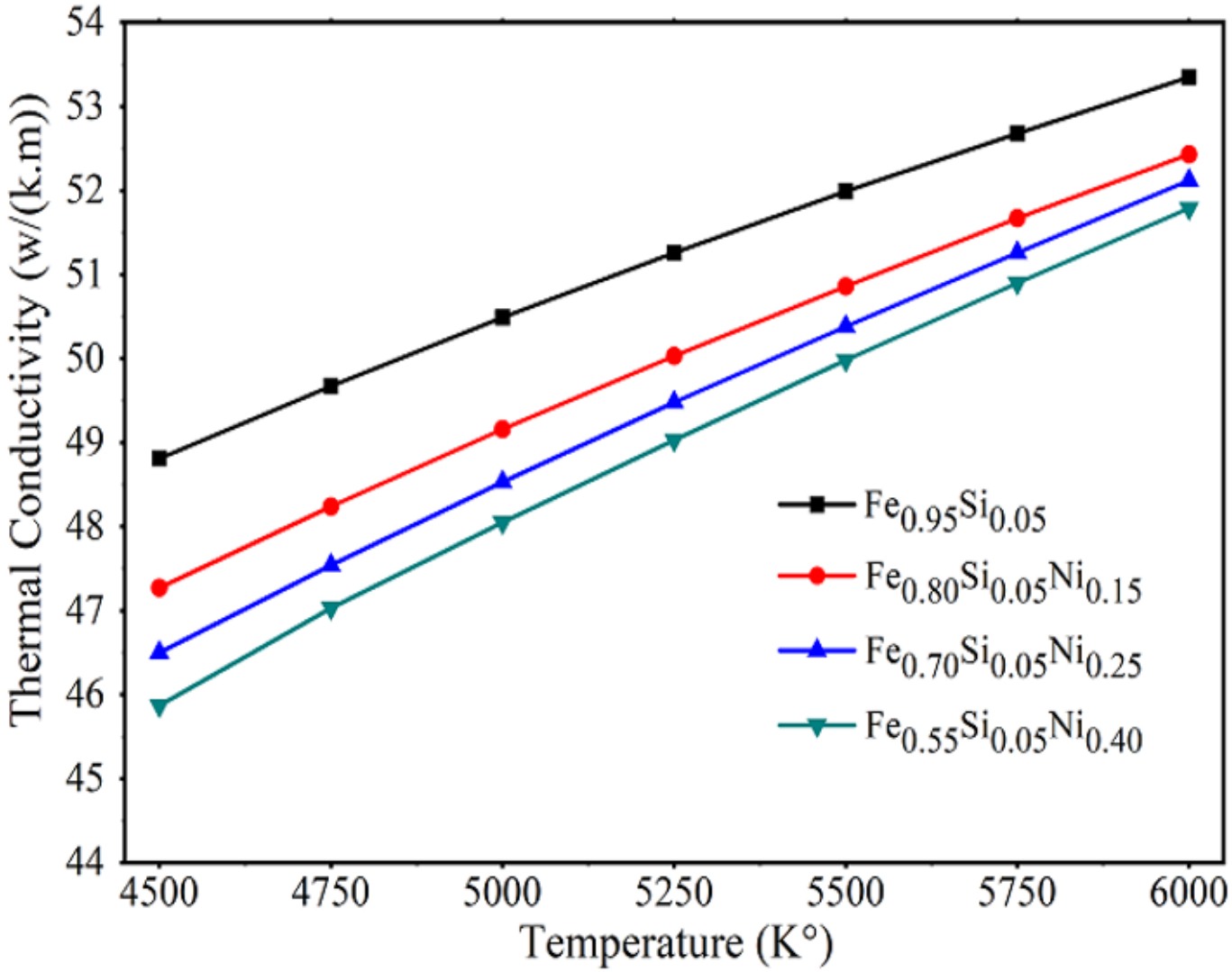

Figure 7

Thermal Conductivity vs temperature at 360 GPa for impurity concentrations of 0%, 15%, 25% and 40% of Ni doped in Fe0.95-xSi0.05Nix of hcp structure.